Investigation of Rock Matrix Retention Properties — Supporting Laboratory Studies II: Diffusion Coefficient and Permeability

Mikko Voutilainen, Jussi Ikonen, Juuso Sammaljärvi,

Marja Siitari-Kauppi, Antero Lindberg, Jukka Kuva,

Jussi Timonen, Martin Löfgren

December 2018

Investigation of Rock Matrix Retention Properties — Supporting Laboratory Studies II: Diffusion Coefficient and Permeability

Mikko Voutilainen, Jussi Ikonen, Juuso Sammaljärvi, Marja Siitari-Kauppi

University of Helsinki, Department of Chemistry - Radiochemistry

Antero Lindberg

Geological Survey of Finland

Jukka Kuva, Jussi Timonen

University of Jyväskylä, Department of Physics

Martin Löfgren

Niressa AB

December 2018

INVESTIGATION OF ROCK MATRIX RETENTION PROPERTIES – SUPPORTING LABORATORY STUDIES II: DIFFUSION COEFFICIENT AND PERMEABILITY

ABSTRACT

Spent fuel from nuclear power plants in Finland will be deposited deep in the crystalline bedrock. To properly estimate the safety of such a repository, the transport properties of the bedrock must be investigated. As a part of such an investigation, a project called rock matrix REtention PROperties (REPRO) has been launched. The project consists of in situ transport measurements and supporting laboratory studies to which this report belongs.

In this study diffusion measurements performed on REPRO rock samples using the water phase through-diffusion measurements with HTO and ^{36}Cl, the gas phase through-diffusion measurements, electrical conductivity measurements and Cl out-diffusion measurements are compiled together to gain deeper knowledge and understanding on the transport properties of the rock and the factors affecting it. This study aims to assist the analysis of the REPRO in situ experiments and to produce data which can be used when comparing the results from the in situ experiments to those from the laboratory experiments. The samples were divided in two groups according to the rock type:veined gneiss (VGN) and pegmatitic granite (PGR) and veined gneiss samples further to three groups according to the in situ experiment they were linked to: Through Diffusion experiment (TDE) that was performed in ONK-PP-324,326 and 327 drill holes, Water Phase Diffusion Experiment (WPDE) that was performed in ONK-PP-323 drill hole and Other VGN samples from ONK-PP-319 drill hole.

The effective diffusion coefficient (D_e) of HTO as error weighted averages over different sample groups were $(1.7 \pm 0.2) \times 10^{-13}$ m^2/s (WPDE), $(3.9 \pm 0.4) \times 10^{-13}$ m^2/s (TDE), $(5.7 \pm 0.7) \times 10^{-13}$ m^2/s (PGR) and $(1.3 \pm 0.1) \times 10^{-13}$ m^2/s (Other). The D_e values of ^{36}Cl were $(0.05 \pm 0.03) \times 10^{-13}$ m^2/s (WPDE), $(3.4 \pm 0.5) \times 10^{-13}$ m^2/s (TDE), $(5.0 \pm 1.0) \times 10^{-13}$ m^2/s (PGR), and $(0.07 \pm 0.03) \times 10^{-13}$ m^2/s (Other). The effective diffusion coefficients from He-gas through-diffusion experiments presented by correcting to the water phase by a factor of 11 000 were $(0.51 \pm 0.03) \times 10^{-13}$ m^2/s (WPDE), $(1.0 \pm 0.1) \times 10^{-13}$ m^2/s (TDE), $(5.0 \pm 0.3) \times 10^{-13}$ m^2/s (PGR), and $(2.0 \pm 0.2) \times 10^{-13}$ m^2/s (Other). The diffusivities were also calculated from the formation factor which was determined from the electrical conductivity measurements and they were $(3.4 \pm 1.1) \times 10^{-13}$ m^2/s (WPDE), $(5.9 \pm 0.5) \times 10^{-13}$ m^2/s (TDE), $(11 \pm 1) \times 10^{-13}$ m^2/s (PGR), and $(1.6 \pm 0.2) \times 10^{-13}$ m^2/s (Other). The last De values were measured from natural chloride out-diffusion experiment being $(0.6 \pm 0.3) \times 10^{-13}$ m^2/s (WPDE), $(2.9 \pm 0.5) \times 10^{-13}$ m^2/s (PGR), $(1.0 \pm 0.3) \times 10^{-13}$ m^2/s (Other).

The effect of anion exclusion was clearly seen on veined gneiss samples when comparing the results of HTO and ^{36}Cl from the through-diffusion experiment in the water phase. This effect was notable in WPDE samples, where the foliation was found to be perpendicular to the direction of diffusion. All of the TDE samples were however highly foliated and the foliation was found to be parallel in the direction of diffusion, which made the diffusion of the elements faster. Due to this, the anion exclusion effect is not as pronounced in TDE as in WPDE. The diffusivities from the He through-diffusion experiments which were performed in the gas phase were systematically lower than the

diffusivities of HTO measured in the water phase in the case of veined gneiss (WPDE, TDE and Other groups). This might be due to the effect of Knudsen diffusion in the veined gneiss samples indicating nano- to micrometer scale pores in the connective porosity of these rocks. Neither anion exclusion nor Knudsen diffusion affected the pegmatitic granite samples in which rock type the connected porosity was formed by intra- and intergranular fissures and fractures in and around of large mineral grains. The electrical conductivity measurements generally overestimated the diffusivities. These diffusivities were determined from the formation factor and yielded the highest values for the PGR due to its more open and direct diffusion routes in the grain boundaries when compared with VGN. The out-diffusion measurements yielded results that were in fair agreement with the other methods.

KIVIMATRIISIN PIDÄTYSOMINAISUUKSIEN TUTKIMUSTA TUKEVAT LABORATORIOTUTKIMUKSET II: DIFFUUSIOKERROIN JA PERMEABILITEETTI

TIIVISTELMÄ

Ydinvoimaloiden jätteenä syntyvä käytetty ydinpolttoaine tullaan loppusijoittamaan Suomessa syvälle kiteiseen peruskallioon. Loppusijoitustilan turvallisuusanalyysejä varten on tärkeää tutkia peruskallion kulkeutumisominaisuuksia. Osana kulkeutumisominaisuuksien tutkimuksia käynnistettiin REPRO-projekti (rock matrix REtention PROperties, kivimatriisin pidättämisominaisuudet). Projekti koostuu useista ONKALO:ssa suoritettavista in situ kokeista ja niitä tukevista laboratoriokokeista, joita tämä työ käsittelee.

Tässä työssä suoritettiin diffuusiokokeita Olkiluodon kivinäytteille käyttäen perinteisiä läpidiffuusiomittauksia kaasu- ja vesifaasissa, sähkönjohtokykymittauksia ja Cl:n ulosdiffuusiokokeita. Vesifaasissa suoritetuissa läpidiffuusiokeissa käytettiin merkkiaineena HTO:ta ja ^{36}Cl-:ta, ja kaasufaasissa heliumia. Työn tuloksena saatiin tärkeää tietoa Olkiluodon peruskallion kulkeutumisominaisuuksista ja niihin vaikuttavista kiven huokosrakenteesta. Yhtenä tämän työn tavoitteena on tuottaa tuloksia, joita voidaan käyttää hyväksi analysoitaessa REPRO-projektissa suoritettavien in situ kokeiden tuloksia, ja joiden perusteella voidaan arvioida laboratoriokokeiden luotettavuutta tuotettaessa parametreja turvallisuusanalyysin tarpeisiin. Tutkitut näytteen jaettiin kahteen ryhmään kivityypin perusteella (juonigneissi, VGN, ja pegmatiittigraniitti, PGR) ja juonigneissinäytteet edelleen kolmeen ryhmään niitä vastaavien in situ kokeiden mukaan: Läpidiffuusio koe (TDE, Through Diffusion Experiment), vesifaasissa suoritettava matriisidiffuusiokoe (WPDE, Water Phase Diffusion Experiment) ja muut juonigneissinäytteet (other). Eri menetelmillä saatiin virheillä painotetuiksi HTO:n efektiivisiksi diffuusiokertoimiksi: $(1.7 \pm 0.2) \times 10^{-13}$ m^2/s (WPDE), $(3.9 \pm 0.4) \times 10^{-13}$ m^2/s (TDE), $(5.7 \pm 0.7) \times 10^{-13}$ m^2/s (PGR) ja $(1.3 \pm 0.1) \times 10^{-13}$ m^2/s (Other). Vastaavasti ^{36}Cl:n efektiivisiksi diffuusiokertoimiksi saatiin: $(0.05 \pm 0.03) \times 10^{-13}$ m^2/s (WPDE), $(3.4 \pm 0.5) \times 10^{-13}$ m^2/s (TDE), $(5.0 \pm 1.0) \times 10^{-13}$ m^2/s (PGR), ja $(0.07 \pm 0.03) \times 10^{-13}$ m^2/s (Other). He-kaasun läpidiffuusiokokeista saatiin vesifaasiin korjatuiksi efektiivisiksi diffuusiokertoimiksi: $(0.51 \pm 0.03) \times 10^{-13}$ m^2/s (WPDE), $(1.0 \pm 0.1) \times 10^{-13}$ m^2/s (TDE), $(5.0 \pm 0.3) \times 10^{-13}$ m^2/s (PGR), ja $(2.0 \pm 0.2) \times 10^{-13}$ m^2/s (Other). Sähkönjohtokykyyn perustuvista formaatiokerroinmittauksista saatiin efektiivisikiksi diffuusiokertoimiksi: $(3.4 \pm 1.1) \times 10^{-13}$ m^2/s (WPDE), $(5.9 \pm 0.5) \times 10^{-13}$ m^2/s (TDE), $(11 \pm 1) \times 10^{-13}$ m^2/s (PGR), ja $(1.6 \pm 0.2) \times 10^{-13}$ m^2/s (other). Vastaavasti kloorin ulosdiffuusiokokeista efektiivisiksi diffuusiokertoimiksi saatiin: $(0.6 \pm 0.3) \times 10^{-13}$ m^2/s (WPDE), $(2.9 \pm 0.5) \times 10^{-13}$ m^2/s (PGR), ja $(1.0 \pm 0.3) \times 10^{-13}$ m^2/s (Other).

Juonigneissinäytteille HTO:lla ja ^{36}Cl:lla saaduissa tuloksissa havaittiin anioniekskluusion aiheuttama vaikutus. Etenkin WPDE-näytteissä tämä vaikutus on vahvasti esillä, sillä näytteissä pääkulkeutumissuunta oli suuntautuneisuutta vastaan kohtisuorassa. TDE-näytteillä tehdyissä kokeissa pääkulkeutumissuunta oli suuntautuneisuuden kanssa samansuuntainen, mikä vähentää diffuusioreittien tortuositeettia verrattuna WPDE näytteisiin. Näin ollen TDE-näytteissä anioniekluusion vaikutus on heikompi. Vastaaville näytteille suoritetuissa kaasufaasimittauksissa havaittiin puolestaan Knudsenin diffuusion aiheuttama vaikutus. Kumpaakaan näistä

ilmiöistä ei havaittu pegmatiittigraniitti näytteille tehdyissä mittauksissa. Pegmatiittigraniitissa mineraalikiteet ovat kooltaan noin 0.5 -2 cm ja johtava huokoisuus koostuu kiteitä halkovista fissuureista, joten diffuusioreittien tortuositeetti on vähäinen. Sähkönjohtokykymittauksista saatujen tulosten havaittiin yliarvioivan efektiivisiä diffuusiokertoimia noin tekijällä kaksi ja ulosdiffuusiomittauksista saadut tulokset olivat yhteneväisiä perinteisistä läpidiffuusiomittauksista saatujen tulosten kanssa.

Avainsanat: Kiteinen kivi, efektiivinen diffuusiokerroin, permeabliteetti. formaatiotekijä, huokoisuus, anioniekskluusio, juonigneissi, pegmatiittigraniitti, REPRO-projekti

TABLE OF CONTENTS

1 INTRODUCTION

The spent fuel from nuclear power plants will be deposited in geological formations. Understanding the nature of the radionuclide transport through geological barriers is essential in any assessment of the confining properties of such barriers. Radionuclide migration within a rock matrix under natural long-term conditions is a complex process controlled by many parameters. Physical parameters such as porosity, hydraulic conductivity and diffusivity are used to describe the transport properties of elements. Typically in natural rock matrices these properties are linked to parameters defining microscopic pore structure, such as pore size distribution, connectivity, tortuosity and constrictivity and by the petrological and chemical nature and charge of the mineral surfaces. In addition, it is essential to link the mineralogy of the rock with the physical and chemical properties mentioned above. An overall characterization of heterogeneous rock structures is required in order to understand the transport processes of radionuclides.

For understanding the microstructural, petrographic-chemical and rock-phase-specific features when interpreting the in situ transport properties, a qualitative and quantitative assessment is needed of:

1. Mineralogy and petrography of the rock
2. Pore space parameters (bulk porosity, spatial porosity distribution, connectivity, anisotropy, heterogeneity, porosity profile, pore size distribution)
3. Hydraulic conductivity parameters
4. Diffusion properties (apparent/effective diffusion coefficient, diffusion pathways, dependence on the probe molecules used)
5. Retardation properties (size, accessibility, distribution of rock-phase specific internal surfaces)

This work focuses on laboratory-based experiments on the drill core samples from the site of in situ experiments at ONKALO, Olkiluoto. The project is called REPROlab from the main project Investigation of Rock Matrix REtention PROperties In Situ. The aim of this report is to aid the interpretation of the results from REPRO in situ experiments (Voutilainen et al. 2014, Poteri et al. 2016) and compare them with those obtained from laboratory experiments to investigate the effect of the environment on the results. This comparison has already been done within the REPRO project (Sammaljärvi et al. 2016, Voutilainen et al. 2016), but only for a limited amount of samples.

The mineralogy and petrography of the Olkiluoto bedrock and samples from the REPRO site has already been widely studied (e.g. Kärki and Paulamäki 2006, Toropainen 2012, Kuva et al. 2012, Ikonen et al. 2015, Sammaljärvi et al. 2017) as well as the porosity (e.g. Ikonen et al. 2015, Kuva et al. 2015) and the diffusion properties (e.g. Kuva et al. 2015, Kuva et al. 2016). This report aims to combine the results of different diffusion coefficient measurements to improve the understanding about the diffusion properties of the rock types used in the REPRO project and the differences between the results of different methods.

The first part of this report (Ikonen et al. 2015) focused on mineralogy and porosity. The report was then complemented by the work by Sammaljärvi et al. (2017). It was found that fine to medium grained veined gneiss samples (biotite rich and altered minerals) had on average a higher porosity and a higher variance of porosity than coarse grained pegmatitic granite (biotite poor) samples. The veined gneiss samples also had small minerals grains with high porosity that contribute only a little to total porosity due to their limited size, but are thought to have a major effect on the diffusion properties of the rock due to their structure, especially if they are well connected (Sammaljärvi et al. 2017). Investigating this connection between the mineralogy and diffusion properties of rock is one of the goals of the project. This report focuses on the diffusion properties of rock, which are important for the safety case of nuclear waste disposal. One of the main retention mechanisms of radionuclides is matrix diffusion from water conducting fractures into the surrounding rock matrix.

There are several ways to measure diffusion properties, in the gas phase (Väätäinen et al. 1993, Hartikainen et al. 1994, 1995, 1996, Kuva et al. 2015) or in the water phase (Neretnieks 1980, Siitari-Kauppi et al. 1994, Johansson et al. 1998). In water phase, the electrical conductivity and through-electromigration experiments can also be used (Löfgren and Neretnieks 2006). When the properties of pore water are investigated with out-diffusion experiments (Eichinger et al. 2006, Eichinger et al. 2010, Eichinger et al. 2013, Voutilainen et al. 2017), the diffusion coefficient of the sample can also be determined. In this report, we combine results obtained by several different methods in order to apply the strengths and to complement the weaknesses of each and gain a more complete picture of the diffusion properties of the rock samples from the REPRO site. We also aim to examine the effect of anion exclusion (Corey et al. 1963), which has been observed in previous experiments in Olkiluoto bedrock (Valkiainen et al. 1995, Kaukonen et al. 1997, Smellie et al. 2014, Voutilainen et al. 2016). The effect of anion exclusion is expected to show especially in samples with a high biotite and clay mineral content, as they contain a significant amount of porosity with nanometer scale apertures and negatively charged mineral surfaces. In the same samples where anion exclusion is prominent, the effects of Knudsen diffusion (Klinkenberg 1941) are also expected, as it is prominent when the pore apertures are low.

2 MATERIALS AND METHODS

2.1 Samples

The drilling and mineralogy of the samples, as well as the sawing diagrams, are described in the first part of this report (Ikonen et al. 2015). Samples from drill cores ONK-PP318, ONK-PP319, ONK-PP321, ONK-PP323, ONK-PP324, ONK-PP326 and ONK-PP327 were used. The same samples used for Ar-pycnometry in the porosity measurements were used for the gas phase diffusion measurements here. All samples had a diameter of roughly 42 mm and a length of 20, 30 or 50 mm for through-diffusion and electrical conductivity experiments and 260-400 mm for the out-diffusion experiments.

Two main rock types present in the samples were veined gneiss (VGN) and pegmatitic granite (PGR). VGN is migmatitic metamorphic gneiss which contains migmatites with vein-like, elongated leucosomes (Kärki and Paulamäki 2006). VGN is fine to medium grained biotite rich rock. The main minerals are biotite, quartz, potassium feldspar and plagioclase, with a significant amount (>10 %) of alteration products and accessory minerals, such as muscovite, chlorite, cordierite, sillimanite, epidote, garnet and opaque minerals. The VGN samples are very heterogeneous and anisotropic and have a significant amount of the porosity with both micro- and nanometre scale pore apertures which are highly tortuous (Sammaljärvi et al. 2017). The porosities of the REPRO VGN samples are typically 0.5 – 1.0 %.

PGR consists of leucocratic, coarse grained (grain size 4-10 mm) rock. The main minerals are quartz, plagioclase and potassium feldspar. There is however only low amount of alteration products, mostly sericite from plagioclase alteration. PGR is heterogeneous, porosity is composed of micro fissures transecting the mineral grains and diffusion pathways are less tortuous than in VGN (Sammaljärvi et al. 2017). The porosities of the REPRO PGR samples are typically 0.4 – 0.6 %.

The samples of this study were divided into four categories according to the rock type and the location if the samples were drilled from the vicinity of in situ experiment. WPDE samples, which correspond to the in situ Water Phase Diffusion Experiment (ONK-PP323), TDE samples, which correspond to the in situ Through-diffusion Experiment (ONK-PP324, ONK-PP326, ONK-PP327), PGR samples (ONK-PP318), and other REPRO samples (ONK-PP319, ONK-PP321). The rock type of WPDE and TDE samples is VGN. Results for mineralogy and porosity for these samples obtained in the first part of the report (Ikonen et al. 2015) are listed in Table 1.

Table 1. *Porosities and rock types obtained for the different REPRO sample groups by Ikonen et al. 2015.*

		Technique	Number of samples	Min / %	Max / %	Average / %
WPDE Samples, (main rock type VGN)		Water gravimetry	3	0.14	0.71	**0.36**
		C-14-PMMA	5	0.30	1.2	**0.62**
		Ar pycnometry	2	0.60	1.3	**0.93**
		All techniques	**10**	**0.30**	**1.3**	**0.73**
TDE Samples (main rock type VGN)		Water gravimetry	6	0.34	1.37	0.79
		C-14-PMMA	3	0.41	1.49	0.88
		Ar pycnometry	3	0.6	3.0	1.54
		All techniques	**12**	**0.34**	**3.0**	**1.07**
PGR Samples		Water gravimetry	2	0.30	0.63	0.43
		C-14-PMMA	3	0.30	0.70	0.50
		Ar pycnometry	3	0.39	0.75	0.57
		All techniques	**8**	**0.30**	**0.75**	**0.50**
Other samples (main rock type VGN)		Water gravimetry	5	0.14	0.71	0.36
		C-14-PMMA	5	0.30	0.40	0.34
		Ar pycnometry	3	0.29	2.60	1.17
		All techniques	**13**	**0.14**	**2.60**	**0.62**

For the gas phase measurements, the samples were dried in a vacuum oven in 50 ºC for several months and kept in a nitrogen atmosphere for 20 minutes before opening the oven to prevent moisture from the laboratory air intruding the pores.

For the electrical conductivity measurements the cylinder edges of the rock core samples were coated with epoxy resin to prevent a conducting electrolyte layer from forming on the sample surface and the ends of the samples were kept uncoated. The samples were dried in an oven in 105 ºC for three days and immersed in the electrolyte for six weeks. When changing the electrolyte between measurements the samples were again dried for three days in 105 ºC. According to Ikonen et. al. 2015 two to three days of drying is sufficient. Dry samples were put in a vacuum chamber and electrolyte was introduced in low pressure conditions so that it evaporated in the chamber. The samples were then kept in low pressure conditions for two hours before the electrolyte immersion and kept

immersed for two weeks before measurements. When the change was made from a stronger electrolyte to a weaker one, the samples were first immersed in deionized water before drying.

2.2   Through-diffusion measurements in water phase

The water phase through-diffusion measurements were done using a sample holder depicted in Fig. 1. The edges of the sample were sealed and the sample was placed in the sample holder in such a way that the ends of the samples were in contact with the chambers. At the beginning of the experiment, a tracer cocktail with HTO and Cl-36 was injected into the injection chamber. During the measurement, the flushing chamber was emptied every or every second week (depending on the sample) and the concentration of HTO and Cl-36 were measured from it using a liquid scintillation counter (Tri-Carb 2910 TR). This way the tracer concentration in the low concentration chamber was always practically zero. The sample holders together with samples were placed in an orbital shaker to ensure an even distribution of the tracers. The tracer concentrations from the samples were measured using a liquid scintillation counter.
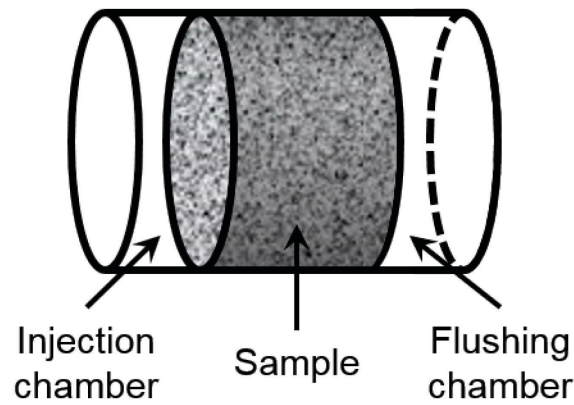

Figure 1. *Schematic of the measurement setup for the through-diffusion measurements in the water phase. Edges of the samples were sealed and the ends were in contact with the injection (high concentration) and flushing (low concentration) chambers.*

The obtained breakthrough curve was modeled by fitting it to the analytical solution obtained from Fick's second law with suitable initial and boundary conditions:

$$\frac{\dot{m}}{m_0} = \sum_{n=1}^{\infty} \frac{\lambda_n}{\sin \lambda_n} \cdot \frac{2D_e H^2}{\rho \cdot (\lambda_n^2 + (LH)^2 + LH)} e^{-\frac{D_e \lambda_n^2}{L^2} t} \tag{1}$$

where $\dot{m}$ is mass flow, m_0 is the initial mass, $0 < \lambda_1 < \lambda_2 < \dots$ are the positive roots of $\lambda \tan \lambda = LH$, D_e is the effective diffusion coefficient, $H = \varepsilon A/V$, ε is the sample porosity, A is the cross-sectional area of the sample, V is the volume of the injection chamber, and L is the length of the sample. In the analysis, least-square fitting was done by treating the effective diffusion coefficient and porosity as the fitting parameters. The porosity is mainly determined by the early part of the breakthrough curve and the diffusion

coefficient is mainly determined by the late-time behavior of the breakthrough curve, which is rather insensitive to small fluctuations in the data collection due to the relative activity flux approach used here. Previously, such analyses have been performed using cumulated data that is proner to these fluctuations than the relative activity flux approach applied here. A representative fit to measured data for sample ONK-PP323 19.00-19.02m is shown in Fig. 2.
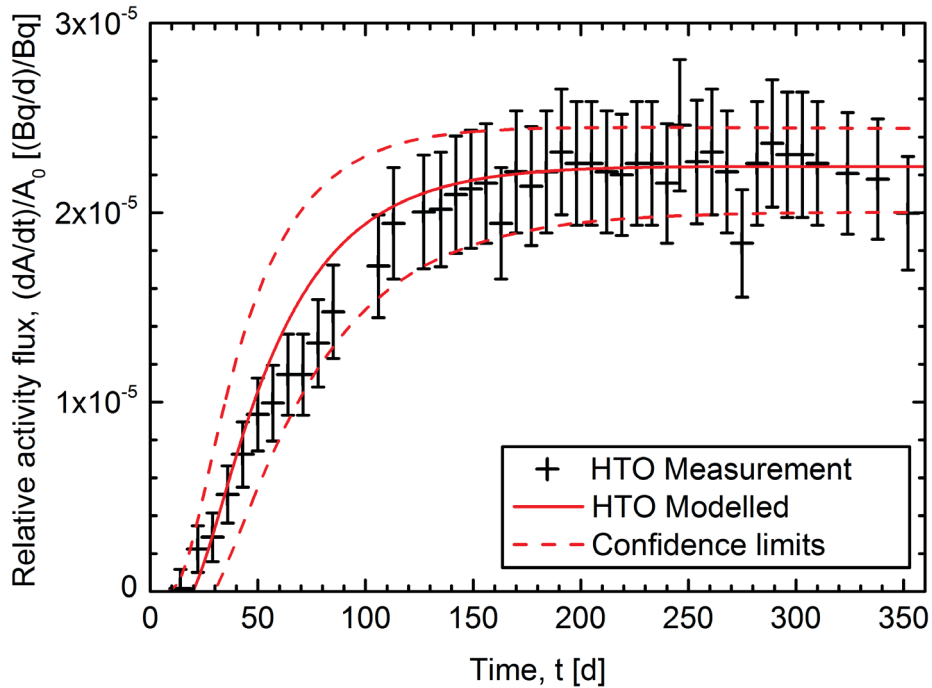

Figure 2. A breakthrough curve of HTO for sample ONK-PP323 19.00-19.02m with ε = (1.1 ± 0.1) % determined from the early part (increasing activity flux) of the curve and $D_e = (1.6 ± 0.3) \cdot 10^{-13}$ m²/s determined from the late part (constant activity flux) of the curve.

2.3 Helium gas methods

The gas phase through-diffusion measurements were used due to them being about four orders of magnitude faster than the water phase measurements. The major aim of the gas phase experiments was to study if they can be used reliably for measuring effective diffusion coefficients instead of the time consuming water phase experiments. In addition, the gas phase measurements give information about the long time behaviour of the breakthrough curves that is not possible study using the water phase through-diffusion experiments. Furthermore, the diffusion experiments performed using different tracer atoms and molecules can be used to get further information on the pore apertures in the rock.The gas phase experiments ignore all the chemistry related to the more realistic water phase measurements, but are fast and the results can be converted to the water phase to mimic the behaviour of conservative tracers such as HTO (Kuva et al. 2015).

2.3.1   Through-diffusion measurements using helium

The effective diffusion coefficient and permeability were measured using a gas phase system where nitrogen is used as the carrier gas and helium as the tracer (Hartikainen et al. 1996, Hartikainen et al. 1998, Kuva et al. 2015). The equipment shown in Figure 3 consists of a sample holder, an injection valve, a He-mass spectrometer, a gas-flow meter, two pressure gauges, and several valves that also connect the setup with nitrogen and helium outlets and a vacuum pump. The injection valve can be used with several injection loops of different volumes. The selection valve is used to connect the injection chamber with the injection valve, the vacuum pump or directly to the helium source, the last of which is done in the permeability measurements. The He-mass spectrometer data are recorded on a PC using LabView-based software. The sample is attached to the sample holder using a commercial butyl rubber sealant band in such a way that only the flat ends of a cylindrical sample are left in contact with the measurement.
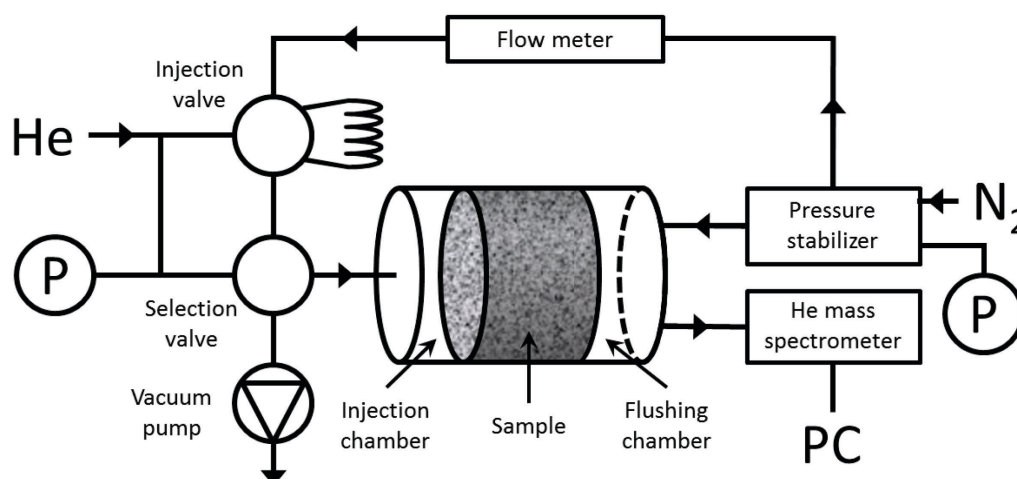

Figure 3. A layout of the through-diffusion equipment. It consists of a sample holder, an injection valve, a He-mass spectrometer, a gas-flow meter, two pressure gauges (P) and several valves that also connect the setup with nitrogen (N_2) and helium (He) outlets and a vacuum pump. (Kuva et al. 2015)

In the through-diffusion measurements, the injection chamber was first connected to a vacuum pump and evacuated, meanwhile a 5 ml loop connected to the injector was filled with helium. The helium was then injected into the injection chamber. Integration of the flow-data for nitrogen replacing the helium in the loop gave the exact amount of the injected helium. Helium then diffused through the sample into the flushing chamber that was continuously flushed with nitrogen, and the flux of helium was determined from a varying helium content of the flushing nitrogen. The pressure in the flushing chamber was kept slightly above the ambient pressure to guarantee no helium was leaked into the flushing chamber from the laboratory. The pressure gauge, flow-rate and He-mass spectrometer data were recorded on PC for later analysis. The breakthrough curve was modeled by again fitting to Eq. (1), this time using only the diffusion coefficient as a fitting parameter. Porosities were measured separately using an Argon pycnometer (Ikonen et al. 2015). A representative fit to measured data for sample ONK-PP318 15.76–15.81m is shown in Fig. 4.
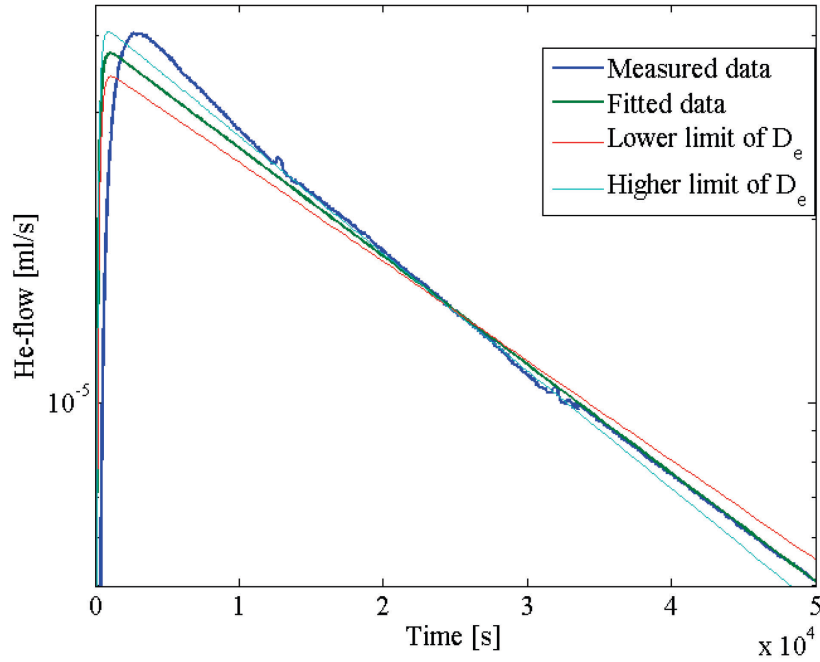
Figure 4. A breakthrough curve of helium for sample ONK-PP318 15.76–15.81m with measured porosity (ε = (0.44 ± 0.14) %) and D_e = (5.7 ± 0.5) · 10^{-9} m^2/s determined from the late part (decreasing He-flow) of the curve. Early part of the measured curve is affected by the injection system and thus measured porosity value was used and the agreement between measured and fitted data is not perfect. This does not, however, affect the late part of the curve and the effective diffusion coefficient can be realiably determined. (Kuva et al. 2015)

2.3.2   Permeability measurements using helium

In the permeability measurements, the helium source was directly connected to the injection chamber and the pressure in both chambers was controlled while flushing the flushing chamber with nitrogen. Pressure of the injection chamber was increased by regular increments, and all pressures and the helium flow were measured after all these values had stabilized. The pressure difference across the sample was typically varied from 20 to 90 kPa.

The permeability measurement was modelled by obtaining helium flux – injection pressure – flushing pressure data points for each pressure difference and then fitting them to

$$Q = Q_{diff} + \frac{kA}{\mu L}\frac{(P_2^2 - P_1^2)}{2P_2},$$
(2)

where Q is the total helium flux, Q_{diff} is the flux caused by diffusion, k is the permeability coefficient, A is the cross-sectional area of the sample, μ is the dynamic viscosity of helium, L is the length of the sample and P_1 and P_2 are the pressures of the flushing chamber and injection chamber, respectively. Permeability coefficient k was thus obtained as the slope of a linear fit.

2.4   Electrical conductivity measurements

When investigating rock transport properties in the water phase, it is possible to speed up the measurements by using an electric potential gradient over the sample. This can be done by measuring the resistivity of the sample and using it to determine a formation factor and finally an effective diffusion coefficient. This yields effective diffusion coefficients much faster in the water phase than the through-diffusion measurements.

In most rock types, especially those located at RERPO site, a majority of the electrical current is propagated by the ionic conduction of the solutes in the pore water, while the amount of electric current propagated in the mineral grains is insignificant (Brace et al. 1968, Löfgren 2015). Additionally, the electrical charge of the mineral surfaces affects the rock conductivity. Taking this into account, the total conductivity (κ_r) of a rock sample can be approximated by (Waxman and Smits 1968)

$$\kappa_r = F_f \kappa_w + \kappa_s, \qquad\qquad (3)$$

where $F_f = D_e/D_w$ is the so called formation factor, which describes the geometrical restriction of the porous medium compared with migration in unconstrained pore water (D_w), κ_w is the electrical conductivity of the unconstrained pore water and κ_s is the surface conductivity of the rock matrix. The proposed linearity of the relation assumes that the surface conductivity and formation factor are independent of the pore water salinity, thereby assuming that the specifics of the diffuse double layer do not impact significantly the mobility of cations attracted to the mineral surfaces or anions in the bulk pore water due to the minor difference in the double layer depth against the salinity. Deviations from these assumptions should cause deviation from linearity; even if this may be difficult to observe experimentally given other experimental uncertainty.

The electrical conductivity measurements were made in connection with the through-electromigration (TEM) experiments, involving the migration of ionic tracers through the rock sample. This increased the complexity of the used equipment (Löfgren and Neretnieks 2006). The outcome of the TEM experiments is not further discussed in this report. The equipment used consisted of five Plexiglas tubes (see Fig 5). The sample, saturated with an electrolyte of known electrical conductivity, was placed in the middle tube. The ends of the sample chamber were connected to the electrolyte filled chambers of same κ_w as the pore water. The connections were sealed with silicon rings to prevent a leak of the electrolyte to the sample chamber and a leak of current between the sample and the sample chamber. A teflon dummy was measured as a control sample and there was no significant leaking of the current. Potential electrodes used for measuring the electrical potential drop over the rock were placed in the electrolyte filled chambers near the ends of the rock sample. The chambers containing the anode and cathode were separated by saturated porous filters made from veined gneiss from the Olkiluoto area, that restrict tracer migration to these chambers in the TEM experiments. The anode and cathode chambers were connected to each other with hoses via droplet bottles, that prevent a current connection between the chambers. Mixing between the electrolytes of the anode and cathode chambers was done with a peristaltic pump to prevent the formation of large pH differences between the anode and cathode chambers. The anode, the cathode and potential electrodes were made of platinum.
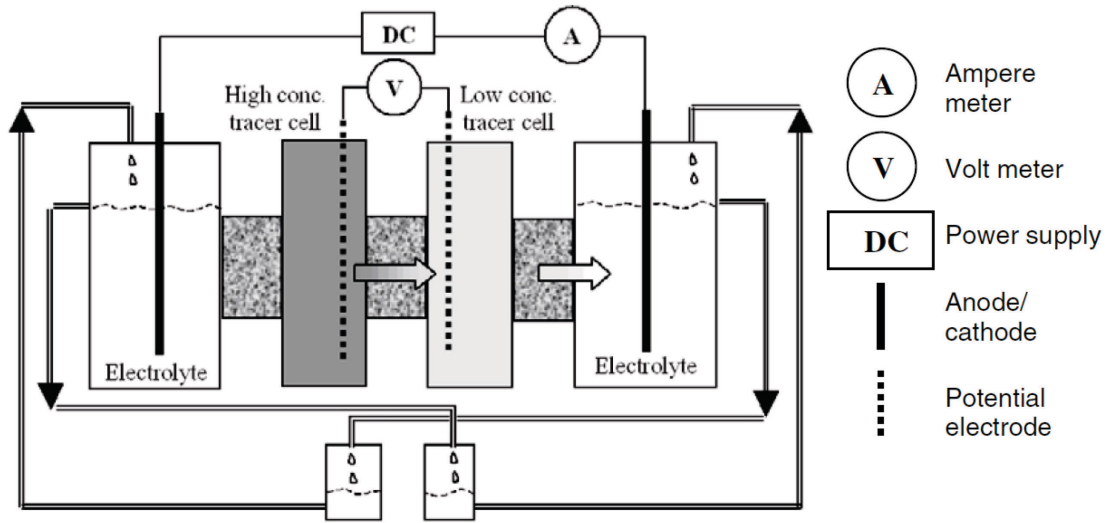
Figure 5. *Schematics of the electromigration experimental setup (Löfgren and Neretnieks 2006).*

The equipment was operated with a computer using LabView 2011 software. The computer was connected to a National Instrument's CompactDAQ (NI-cDAQ-91749) modular data acquisition system which was installed with an AD-module (NI-9208) and a power source / sine wave generator NI-9269. The power source was able to generate a 0-40 V direct current (DC). The current and voltage measurements were done using an USB connected digital multimeter (NI USB-4065). The multimeter was connected to the potential electrodes close to the sample, and to the anode and cathode.

For formation factor measurements, the resistivities of the samples had to be measured. The measurements were done using a 25 V potential drop. Five different electrolytes were used, 0.001 M, 0.01 M, 0.1 M, 0.2 M and 0.5 M NaCl with electrical conductivities of 0.01347 S/m, 0.1717 S/m, 1.122 S/m, 1.905 S/m and 4.684 S/m respectively. The different electrolytes were partly used to investigate if the ionic strength has a major impact on the effective diffusion coefficient. It is assumed that the increasing ionic strength would decrease the thickness of the diffuse double layer on the negatively charged mineral surfaces that causes an electric repulsion of anions. This leads to a larger accessible pore volume for anions and thus decreases the effect of anion exclusion. It is cautioned, though, that relatively small effects of the ionic strength of the pore water on the anion exclusion factor may be masked in the experiments, due to other experimental uncertainty.

Rock resistivity ρ obtained from the measurements was determined by

$$\rho = \frac{A}{l} \cdot \left(\frac{V_D}{I_m} - \left(\frac{2l_w}{\kappa_w A} \right) \right), \tag{4}$$

where A is cross-sectional area of the rock sample, l is the length of the sample, V_D is the electric potential drop over the sample, I_m is the current through the sample, and l_w is the length of the water column between the sample and the potential electrodes in the electrolyte chamber. By plotting the conductivity of the rock sample κ_r versus the

electrical conductivity of the pore water κ_w, the slope of the linear regression line gives the formation factor F_f (see Equation 3). This is under the assumption that neither the formation factor nor the surface conductivity is significantly impacted by the ionic strength of the pore water. If there are cases of clear deviations form linearity, this must be discussed. The formation factor was then converted into an effective diffusion coefficient using

$$D_e = F_f \cdot D_w = F_f \cdot 1.70 \cdot 10^{-9} \frac{m^2}{s},$$ (5)

where the numerical value of D_w reflects that current is propagated by both sodium and chloride ions.

2.5 Chloride out-diffusion experiments from naturally saturated samples

The out-diffusion experiments are presented in more detail in a previous Posiva Report (Voutilainen et al. 2017) and thus the idea is presented here only shortly. The experimental setup is shown in Fig. 6. The samples were vacuum packed after drilling and in the measurement placed in a plastic tube filled with deionized water, which was changed and measured every two weeks.
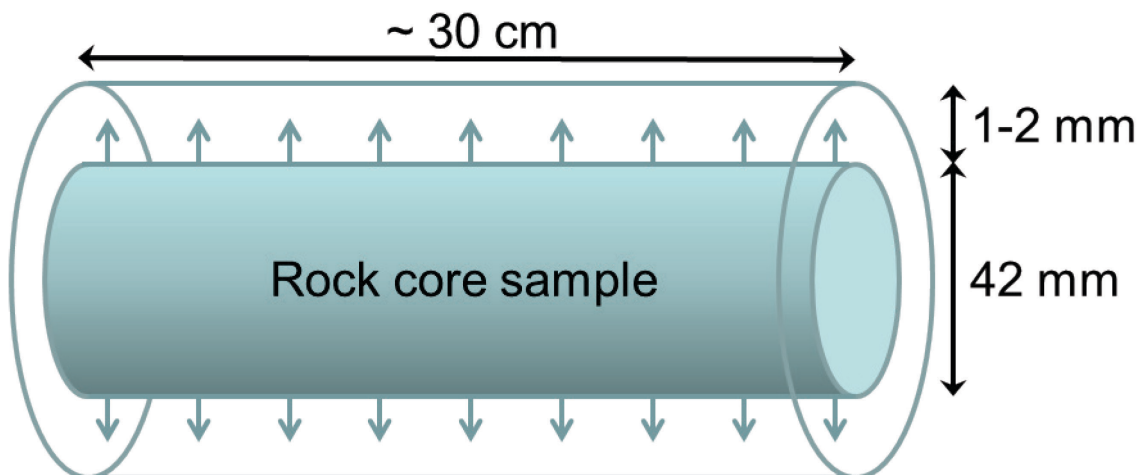

Figure 6. Experimental setup of the out-diffusion experiment. The net flux of elements from naturally saturated rock core samples to the surrounding water reservoir were measured.

In the experiment, the flux of the chloride out from a porous rock sample placed in a container filled with ion changed water is measured. It is assumed that the chloride moves in the rock by diffusion.

The mass of the chloride in the rock sample, m(t), can be written as:

$$m(t) = 4m_0 \sum_{n=1}^{\infty} \frac{1}{\alpha_n^2} e^{-\frac{D_p \alpha_n^2 t}{a^2}}, \tag{6}$$

where $m_0 = \pi a^2 L \varepsilon C_0$ is the mass of chloride in the rock sample at $t = 0$, a is the radius of the sample, L is the length of the sample, ε is the porosity of the rock, C_0 is the chloride concentration at $t = 0$, $\alpha_1 < \alpha_2 < ...$ are the positive zeros of the Bessel function J_0, and D_p is the pore diffusion coefficient of the sample (Voutilainen, et al. 2017). In the experiments, we have measured the outflow of chloride with two week time intervals. The amount of chloride diffusing out of the rock sample in the sampling time interval $[t_i, t_{i+1}]$ is

$$\Delta m_i = m(t_i) - m(t_{i+1}). \tag{7}$$

If we want to use Eq. (7) to interpret measured data, we have two unknown parameters, m_0 and D_a. In order to get rid of the unknown parameter m_0 we consider the ratio d(t) of the outflow of chloride in the time interval $[t, t + \Delta t]$ and in the time interval $[0, t + \Delta t]$:

$$d(t) = \frac{m(t) - m(t + \Delta t)}{m_0 - m(t + \Delta t)}. \tag{8}$$

From the measured data, we get $d(t_i)$ at the times $t_i = i \cdot \Delta t$:

$$d(t_i) = \frac{\Delta m_i}{\sum_{k=1}^{i} \Delta m_k}. \tag{9}$$

Using the coefficient of diffusion as a fitting parameter we fit our model (Eq. (8), using Eq. (6) for m(t)) to the measured data. An example of such a fit is shown in Fig. 7 (left panel).

It was not possible to interpret all of the out-diffusion curves using a homogeneous model as the rock consists of more than one mineral with different transport properties. For these curves, the data was interpreted using a dual component model, where the sample consists of disks of two different materials. The approach can be considered as second order approximation of the real heterogeneous nature. In reality it is expected that the rock consists of multiple components that all have different effect on observed results. However, due to experimental limitations such differences may not be seen within the time scale of the experiment. If we ignore fluxes in the axial direction, we can describe the system with two independent equations for the mass of chloride in the component k in the sample, $m_k(t)$:

$$m_k(t) = 4m_{0,k} \sum_{n=1}^{\infty} \frac{1}{\alpha_n^2} e^{-\frac{D_{pk}\alpha_n^2 t}{a^2}} =: 4m_{0,k}f_k(t). \tag{10}$$

The amount of chloride diffusing out of the rock sample in the time interval $[t_i, t_{i+1}]$ is

$$\Delta m_i = m_1(t_i) + m_2(t_i) - m_1(t_{i+1}) - m_2(t_{i+1}), \tag{11}$$

where $m_0^{(k)} = \pi a^2 L p_k \varepsilon_k C_0$, p_k is the portion of material k in the sample, and ε_k its porosity (Voutilainen et al. 2017). The ratio $d(t)$ now takes the form:

$$d(t) = \frac{f_1(t) - f_1(t + \Delta t) + K(f_2(t) - f_2(t + \Delta t))}{f_1(0) - f_1(t + \Delta t) + K(f_2(0) - f_2(t + \Delta t))}, \tag{12}$$

where

$$K = \frac{p_2 \varepsilon_2}{p_1 \varepsilon_1} = \frac{m_{0,2}}{m_{0,1}} \tag{13}$$

is the ratio of the pore volumes of the materials. In this case, we have three fitting parameters, pore diffusion coefficients D_{p1} and D_{p2}, and the ratio K. D_{p1}, D_{p2}, and K are used as fitting parameters when fitting Eq. (12) to the measured data. An example of such a fit is shown in Fig. 7, right panel. The pore diffusion coefficient was converted to effective diffusion coefficients using the porosities reported by Voutilainen et al. (2017).
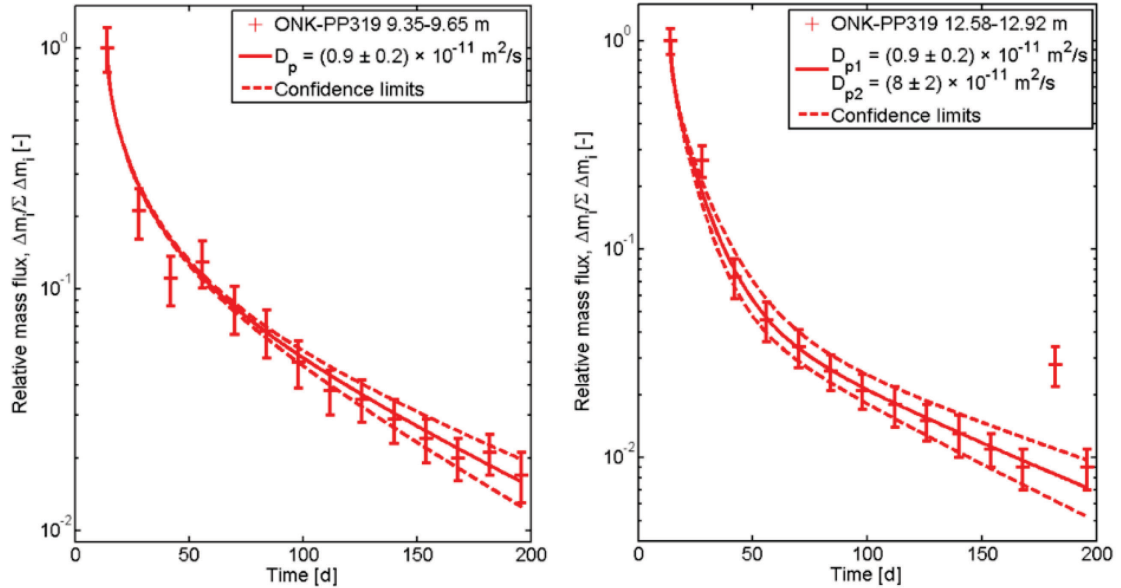

Figure 7. *Measured and fitted out-diffusion curves for sample ONK-PP319 9.35-9.65m using the homogeneous model (left panel) and ONK-PP319 12.58-12.92m using the two component model (right panel). The data is present as relative mass flux from the sample.*

3 RESULTS

3.1 Through-diffusion measurements in water phase

The through-diffusion measurements were conducted in the water phase using HTO and [36]Cl as tracers. These measurements provided baseline results and information on anion exclusion. The results of the water phase through-diffusion measurements are given in Table 2.

Table 2. *Effective diffusion coefficients (D_e) measured in the water phase using HTO and [36]Cl as tracers.*

		Sample	D_e(HTO) × 10^{-13} m²/s	D_e([36]Cl) × 10^{-13} m²/s
WPDE samples	(VGN)	ONK-PP323 18.89-18.94m	2.5 ± 0.3	<1
		ONK-PP323 18.94-18.96m	1.6 ± 0.3	0.05 ± 0.03
		ONK-PP323 18.96-18.98m	1.4 ± 0.2	0.05 ± 0.03
TDE samples	(VGN)	ONK-PP324 11.42-11.44m	3.4 ± 0.6	3.4 ± 0.8
		ONK-PP326 11.35-11.37m	4.8 ± 0.6	3.4 ± 0.7
		ONK-PP327 11.95-11.97m	3.5 ± 0.6	3.4 ± 0.7
PGR samples		ONK-PP318 15.79-15.84m	5.7 ± 0.6	5.0 ± 0.1
Other samples (VGN)		ONK-PP319 9.26-9.31m	2.3 ± 0.4	<1.5
		ONK-PP319 9.31-9.33m	1.3 ± 0.2	0.3 ± 0.2
		ONK-PP319 9.33-9.35m	1.2 ± 0.2	0.06 ± 0.03
		ONK-PP319 12.57-12.59m	1.3 ± 0.2	<1.5
		ONK-PP319 12.83-12.88m	3.0 ± 0.4	<1.5
		ONK-PP319 12.88-12.90m	0.95 ± 0.15	<1.5

For many samples no breakthrough of chloride was observed and thus no diffusion coefficient could be measured. For these samples, an upper limit for the effective diffusion coefficient is given in Table 2.

The experiments were repeated using higher ^{36}Cl concentration by activity. The breakthrough of ^{36}Cl was observed but activity was still close to the detection limit causing high uncertainty in the results. This was interpreted as an effect of anion exclusion that is caused by the differences in the interaction of cations and anions with the pore surfaces. Due to the presence of the nanometer scale pores (micropores >2.5nm, mesopores 2.5-50nm and macropores >50nm), especially in altered clay materials, and the fact that both Cl ions and some mineral surfaces are negatively charged at these conditions, the ions experience repulsion on the mineral surface and thus their migration is hindered in comparison with HTO.

The effect of anion exclusion was clearly seen in the WPDE samples, as the obtained effective diffusivities were significantly smaller for Cl than for HTO. For one WPDE sample and several other VGN samples (ONK-PP319) concentration of ^{36}Cl remained below the detection limit in the flushing chamber and Cl breakthrough was not observed in the experimental set up used here. The finding indicates the influence of anion exclusion since at the same time a clear breakthrough of HTO was measured. Having this in mind, it might have been possible to get a measurable breakthough of ^{36}Cl if higher initial ^{36}Cl was used (exceeds the limits of C-type laboratory) or if a longer collection interval was used (long experimental time). Unexpectedly the TDE samples show no effect of anion exclusion despite having a similar mineral composition as WPDE samples. However, their porosity was higher than that of the WPDE samples (see Table 1), likely arising from higher content of high porosity accessory minerals (pinitized cordirite) and micro fractures with bigger pore apertures than those of WPDE samples (Sammaljärvi et al. 2017). These porous areas formed foliated bands in the rock cores and the diffusion of elements took place parallel to the foliation in TDE samples whereas in the WPDE rock cores the diffusion was perpendicular to foliation. These porous minerals seem to take part on the diffusion in the samples. For the PGR sample the effective diffusion coefficients of HTO and Cl are similar and are not influenced by anion exclusion. This result is in accordance with the structural and mineralogical findings by Sammaljärvi et al. (2017). They found out that the pore apertures of PGR samples from REPRO site are mainly on the micrometer scale and that the samples contain only trace quantities of mica and clay minerals that have negatively charged mineral surfaces and are capable of causing anion exclusion. In General, the results are in good agreement with previously reported values for VGN and PGR samples from Olkiluoto area (Smellie et al., 2014).

3.2 He gas methods

Through-diffusion measurements were also conducted in the gas phase in order to have results with an inert tracer. The measurements were conducted using helium as a tracer in nitrogen atmosphere and are given in Table 3. The permeabilities were also measured in the gas phase and the results are given in Table 3. In order to compare results from the gas phase through-diffusion measurements to the ones from the water phase measurements, it is necessary to convert the gas phase results to the water phase. This conversion was done by using a conversion factor of 11 600 (Kuva et al., 2015). The converted results are presented in Table 3.

The results obtained from the gas phase measurements for the WPDE and TDE samples are lower than those obtained from the water phase measurements by about a factor of four. This is likely caused by Knudsen diffusion (Klinkenberg 1941), a form of diffusion where the particles collide mostly with pore walls instead of each other. Knudsen diffusion becomes prominent when the mean free path of the particles is at least as large as the pore apertures, meaning that it is only relevant in the gas phase measurements on samples with small pore apertures, such as the WPDE and TDE samples. The mean free path of helium atoms is tens of nanometers (50 nm – 100 nm) whereas the pore apertures in the VGN are in micro – (>2.5nm) and meso pores (2.5-50 nm) range, thus it is clear that helium atoms collide to the pore walls. This decreases the diffusivity of the helium atoms and the sum effect is seen as lower effective diffusion coefficients compared with the effective diffusion coefficient of HTO measured by the through diffusion experiments in the water phase. In general, the effect of Knudsen diffusion is very similar to one of anion exclusion: In the micro and meso pores the molecules interact more with the walls of the pores (in respect to pores with micrometers scale apertures) which is then observed as decreased diffusivity. The connected porosity of PGR samples is formed by micro fissures cutting the mineral grains and the fissures have pore apertures from a few micrometers to tens of micrometers and diffusion takes place mainly in these low tortuous micro fissures. Thus Knudsen diffusion is not relevant in PGR samples and the gas phase results are in accordance with the water phase results. The results for the other samples are also in accordance with the water phase measurements. The pore structure and mineral composition of these samples were found to be quite different in comparison with WPDE and TDE samples which explains that Knudsen diffusion does not affect the results of PGR samples (Ikonen et al. 2015, Sammaljärvi et al. 2017). In conclusion, the gas phase through diffusion experiments gave indirect information about the mean pore apertures of different rock samples. In WPDE and other samples considerable amount of pore apertures within the main diffusion are in the nanometer scale whereas in PGR samples the main diffusion routes consist of micrometer scale fissures that are not affected by Knudsen diffusion. The work by Sammaljärvi et al. (2017) reach the same conclusion using C-14-PMMA autoradiography and scanning electron microscopy.

Table 3. *Effective diffusion coefficients (D$_e$(He), D$_e$(H$_2$O)) and permeabilities (k(He)) measured using He-gas methods. The D$_e$(He)results are given for helium in pore space filled by nitrogen and D$_e$(H$_2$O) are converted to the water phase using a conversion factor of 11 600.*

	Sample	D_e(He) × 10^{-9} m²/s	D_e (H₂O) × 10^{-13} m²/s	k(He) × 10^{-19} m²
WPDE samples	ONK-PP323 18.02-18.07m	3 ± 1	2.6 ± 0.9	11.3 ± 0.1
	ONK-PP323 18.83-18.89m	0.58 ± 0.05	0.50 ± 0.05	0.2 ± 0.1
	ONK-PP323 18.94-18.96m	5.4 ± 0.5	4.7 ± 0.5	53 ± 5
	ONK-PP323 19.02-19.07m	0.50 ± 0.05	0.43 ± 0.05	0.14 ± 0.02
	ONK-PP323 20.89-20.91m	0.75 ± 0.10	0.65 ± 0.10	0.9 ± 0.1
TDE samples	ONK-PP324 11.49-11.51m	0.8 ± 0.1	0.69 ± 0.10	3.6 ± 0.4
	ONK-PP326 11.42-11.44m	1.4 ± 0.1	1.21 ± 0.10	2.0 ± 0.2
	ONK-PP326 11.72-11.74m	1.1 ± 0.1	0.95 ± 0.10	9.5 ± 0.2
	ONK-PP327 12.05-12.07m	1.2 ± 0.1	1.03 ± 0.10	0.2 ± 0.1
PGR samples	ONK-PP318 13.92-13.95m	8.2 ± 0.8	7.1 ± 0.7	860 ± 70
	ONK-PP318 13.97-14.02m	3.2 ± 0.6	2.8 ± 0.6	64 ± 1
	ONK-PP318 15.74-15.79m	5.7 ± 0.5	4.9 ± 0.5	5.9 ± 0.2
	ONK-PP318 16.87-16.92m	6.7 ± 0.7	5.8 ± 0.7	9 ± 1
Other samples	ONK-PP319 9.16-9.21m	2.0 ± 0.2	1.7 ± 0.2	1.3 ± 0.2
	ONK-PP319 9.47-9.52m	1.4 ± 0.3	1.2 ± 0.3	6 ± 1
	ONK-PP319 12.46-12.51m	2.8 ± 0.2	2.4 ± 0.2	1.1 ± 0.1
	ONK-PP319 12.70-12.75m	3.8 ± 0.5	3.3 ± 0.5	49 ± 5
	ONK-PP321 10.26-10.31m	1.9 ± 0.7	1.7 ± 0.7	39 ± 1

3.3   Electrical conductivity measurements

Electrical conductivity measurements were conducted to gain another comparison with the other methods in a relatively short time. Formation factors were obtained by measuring the rock resistivity at five different electrolytes, plotting the results and using linear regressions, and determining formation factors from the slope of the linear fit (Eq. 3). The plots are given in Fig. 8. A reasonable data uncertainty assessment has been made for the rock resistivity measurements while it is more difficult to assess the uncertainty in the electrical conductivity of the pore water. Especially when changing the pore water from an electrolyte of higher to lower ionic strength, the removal of the excess ions in the porous system may have been inadequate. This uncertainty may, or may not, give rise to deviations from linearity that mask deviations that originate from the varied ionic strength and its impact on the anion exclusion factor. The resulting formation factors are listed in Table 4 together with the effective diffusion coefficients obtained by Eq. (5). In the Table 4, there is also a note on the linearity of the data.
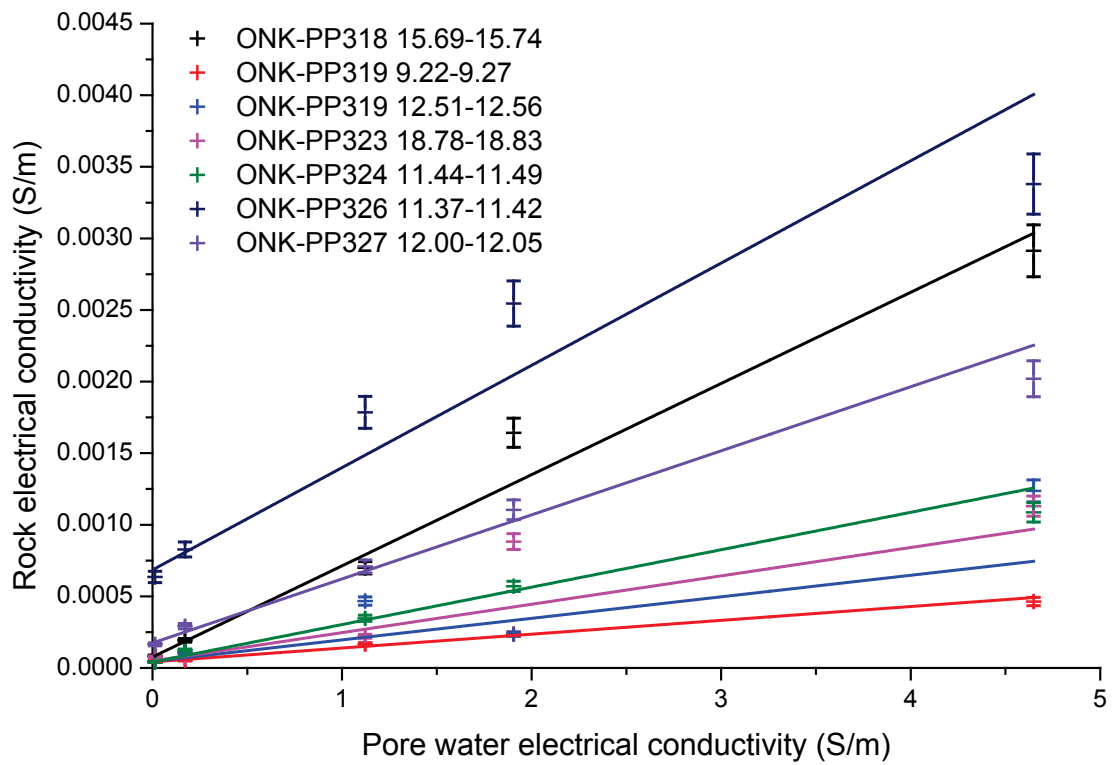
Figure 8. *Rock conductivities as a function of pore water conductivities from electrical conductivity experiments. The solid are linear fits to conductivity data and the slope of the fit gives the formation factor and interception point gives the surface conductivity.*

Table 4. Formation factor and effective diffusivity results obtained by electrical conductivity experiments.

	Sample	$F_f \times 10^{-4}$	$D_e \times 10^{-13}$ m^2/s	*Deviations from linearity and R^2*
WPDE samples	ONK-PP323 18.78-18.83m	2.0 ± 0.7	3.4 ± 1.1	Deviation of fluctuating character, R^2=0.86
TDE samples	ONK-PP324 11.44-11.49m	2.6 ± 0.4	4.4 ± 0.6	Small deviation, R^2=0.99
	ONK-PP326 11.37-11.42m	7.1 ± 1.3	12 ± 3	Deviation with possible indication of effects of ionic strength. Sample has higher κ_s than other samples and also larger evaluated κ_s than measured κ_r at 0.001 M. R^2=0.91
	ONK-PP327 12.00-12.05m	4.5 ± 0.5	7.6 ± 0.7	Small deviation, R^2=0.99
PGR samples	ONK-PP318 15.69-15.74m	6.4 ± 0.6	10.8 ± 1.0	Small deviation of fluctuating character, R^2=0.97
Other samples	ONK-PP319 9.21-9.26m	0.97 ± 0.08	1.6 ± 0.2	Small deviation, R^2=0.99
	ONK-PP319 12.51-12.56m	1.5 ± 0.6	2.6 ± 1.0	Deviation of fluctuating character, R^2=0.89

The obtained effective diffusion coefficients for the WPDE and TDE samples are on average a factor of about two larger than those obtained from the water phase through-diffusion experiments using HTO as the tracer (see Table 2). For example, the samples from drill cores ONK-PP319 and ONK-PP318 the corresponding factor is 1.7 and 1.9, respectively. These results are in line with the previous comparisons of the two methods on rock samples (e.g. Löfgren 2015). The previous comparisons have been performed using samples in which anion exclusion is playing a minor role. According to current knowledge, artefacts that could explain the difference between the methods include: 1. Long range electronic conduction in the mineral lattice, 2. Surface conduction, 3. Short-range electric conduction in metallic minerals that block the nanometer scale pores. The origin and effect of these artefacts are thoroughly introduced and discussed by Löfgren (2015). It appears that surface conductivities, and thus the migration capacity of cations predominately sorbing by cation exchange in the diffusive double layer is larger than in previous measurements on Swedish rock (Löfgren 2015). The higher surface conductivities probably arise from the high biotite content of the samples. In the conditions of the experiments, the biotite grains have negatively charged surfaces that could be responsible for the observed difference in surface conductivity. For some

samples there may be support for an anion exclusion factor that decreases with increasing ionic strength of the pore water. For other samples, this notion is contradicted. However, the method is not very sensitive for studying this matter and possible indications are weak.

3.4   Out-diffusion experiments

The measured chloride out-diffusion curves were first analysed using the homogenous model given in Eq. (8) to determine the effective diffusion coefficients. For two samples (ONK-PP319 9.35-9.65 m and ONK-PP323 17.90-18.20 m) the homogeneous model produced results which were in agreement with the measured data. For the rest of the samples (ONK-PP318 13.85-14.15 m, ONK-PP318 16.75-16.99 m, ONK-PP319 12.58-12.92 m, and ONK-PP321 10.14-10.41 m) the homogeneous model was not able to explain the result. For these samples, the dual component model of Eq. (12) was applied to find a better agreement. At the early part of the out-diffusion curves, the high diffusion coefficient component of the sample dominates and a rapid drop in the mass of incoming chloride is seen. At the late part of the curves, the high diffusion component contains only a small amount of chloride and thus the effect from the lower diffusion coefficient component becomes dominating. Between these two areas there is a convergence area which is seen as a relatively sharp change in the derivatives of the curves. The numerical values from the analysis shown above are given in Table 5. It is assumed here that the higher diffusion coefficients can be compared with the ones other methods because the high diffusion coefficient is likely dominating in the through-diffusion measurements within the centimeter scale.

Table 5. Effective diffusion coefficients (D_e) for the out-diffusion samples. For the data modelled by dual component model the effective diffusion coefficients of both components and the ratio of pore volumes of the components, K, is also given.

	Sample	1. $D_e \times 10^{-13}$ m²/s	2. $D_e \times 10^{-13}$ m²/s	K
WPDE samples	ONK-PP323 17.90-18.20 m	0.6 ± 0.2	-	-
PGR samples	ONK-PP318 13.85-14.15 m	0.3 ± 0.1	5 ± 2	2.7 ± 0.6
PGR samples	ONK-PP318 16.75-16.99 m	0.3 ± 0.1	1.8 ± 0.6	0.70 ± 0.14
Other samples	ONK-PP319 9.35-9.65 m	0.8 ± 0.2	-	-
Other samples	ONK-PP319 12.58-12.92 m	0.6 ± 0.2	6 ± 2	1.1 ± 0.3
Other samples	ONK-PP321 10.14-10.41 m	0.3 ± 0.1	3 ± 1	1.6 ± 0.4

The result obtained for the WPDE sample is in accordance with those obtained by through-diffusion experiments for HTO in the water phase or He in the gas phase. The result is, however, larger than the ones for Cl in the water phase through-diffusion experiments. Here the difference may arise from different types of experiments: In the beginning of the out-diffusion experiment the chloride is located in the pore space of the samples whereas in the through-diffusion experiment the tracer is located at the injection chamber. In the out-diffusion experiment the mean diffusion distance to the chamber around the rock sample is shorter than in the through-diffusion experiment due to the geometry of experimental setup. Hence, the fast diffusion routes (even if they are interconnected only at short distances) bring Cl into the measurement instantly whereas in the through-diffusion experiment the ^{36}Cl has to travel through the whole sample before reaching the measurement chamber. In this regard, the results from through-diffusion experiments represent the averaged diffusion coefficient while the ones from the out-diffusion experiments show also signals from different time scales. It is expected that WPDE sample has a second component with even lower diffusivity. The effect of it, however, is not seen in this time scale and within the detection limit of the measurement. No TDE samples were investigated with this method. Both PGR samples required a two-component model, which was expected according the previous diffusion experiments with large PGR samples (Kuva et al. 2016). Comparison to the water phase results for Cl shows that the components with low diffusivity are lower and the ones with high diffusivity higher than the ones from the through-diffusion measurements (see Tables 2 and 5). This is somewhat obvious as the through-diffusion experiment offers an effective value for the whole sample whereas the out-diffusion experiment is able catch diffusion coefficients dominating in different time scales. A similar behavior was observed for the other samples as well.

3.5   Comparison of the results from all methods

All of the diffusivity results for each sample group are shown in Figs. 9-12. The results are mostly in agreement with each other with some notable exceptions. In following the differences between each sample type is discussed using available information about the pore and mineral structure of the samples.
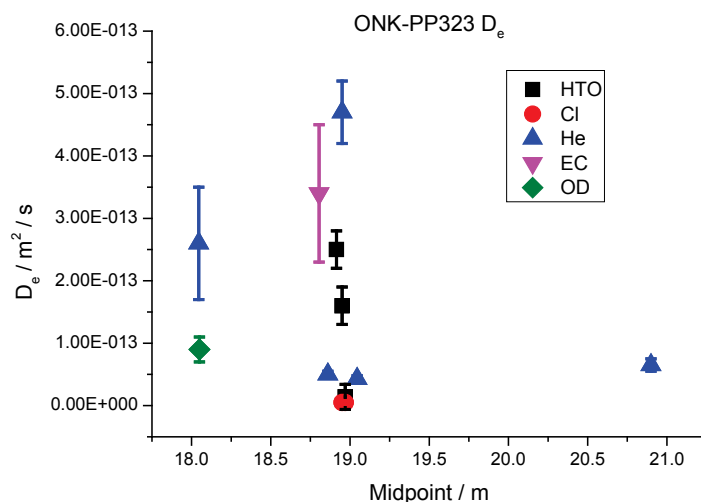
Figure 9. All diffusivity results for the WPDE samples using the water phase (HTO and Cl) and the gas phase (He) through-diffusion experiments, electrical conductivity measurements (EC), and out-diffusion experiments (OD).

The results for the WPDE samples were mostly as expected (see Fig.9). The gas phase results were lower than those obtained from the water phase through-diffusion experiments due to Knudsen diffusion. One of the gas phase results show higher value than the rest of the methods as there were a visible leucosome feature cutting through the sample. The effect of structural heterogeneity causes the high diffusivity here. For the rest of the gas phase results, the Knudsen diffusion was found to be prominent in the WPDE and Other samples that consist of VGN with high biotite content and a significant amount of porosity with micro and meso scale apertures. Biotite has a sheet silicate structure and the distance between sheets is mostly some nanometers. In addition, it has been found that the space between biotite lamellae is filled by clays (Sammaljärvi et al. 2017). Thus anion exclusion might have had a significant effect on the results, which could be seen in lower effective diffusion coefficients for Cl than for HTO. The formation factor measurements slightly overestimated the diffusivity and the out-diffusion measurements gave results that were in accordance with the other methods.

Similar trends were noticeable in the results of the TDE samples (see Fig. 10). The effect of Knudsen diffusion was clearly visible as the gas phase results were systematically lower than the water phase results. This was expected, as the TDE samples also consist mostly of VGN. Anion exclusion was, however, negligible here, as the effective diffusivities were almost equal for two water phase tracers. This was due to the fact that HTO and ^{36}Cl diffused along the foliation which was formed by the porous veins in the TDE samples. Also higher number of the altered minerals were found in the TDE samples than than in WPDE samples (Sammaljärvi et al. 2017) providing diffusion paths with apertures high enough for anion exclusion to disappear but still small enough for Knudsen diffusion. Furthermore, the main diffusion direction in the TDE samples was along the foliation where as in WPDE samples it was against the foliation which might partly explain the absence of anion exclusion in the TDE samples. In the TDE samples there are highly porous veins that go through the sample and some of these contain fissures with relatively high apertures (Ikonen et al. 2015). This might also have an effect to anion

exclusion but it does not explain the gas phase results. On the other hand, the measurements were not performed for exactly the same samples but for samples right next to other. The structural variation in samples might partly explain the difference in the results even though great deal of effort was paid to select visually similar samples for all of the measurements. Furthermore, the samples for the gas measurements have been selected from the same intervals as for other studies. The results of the WPDE and TDE samples from the electrical conductivity measurements were on average larger by a factor of two, compared with the through-diffusion method using HTO as the tracer on nearby samples. No out-diffusion measurements were done on the TDE samples.
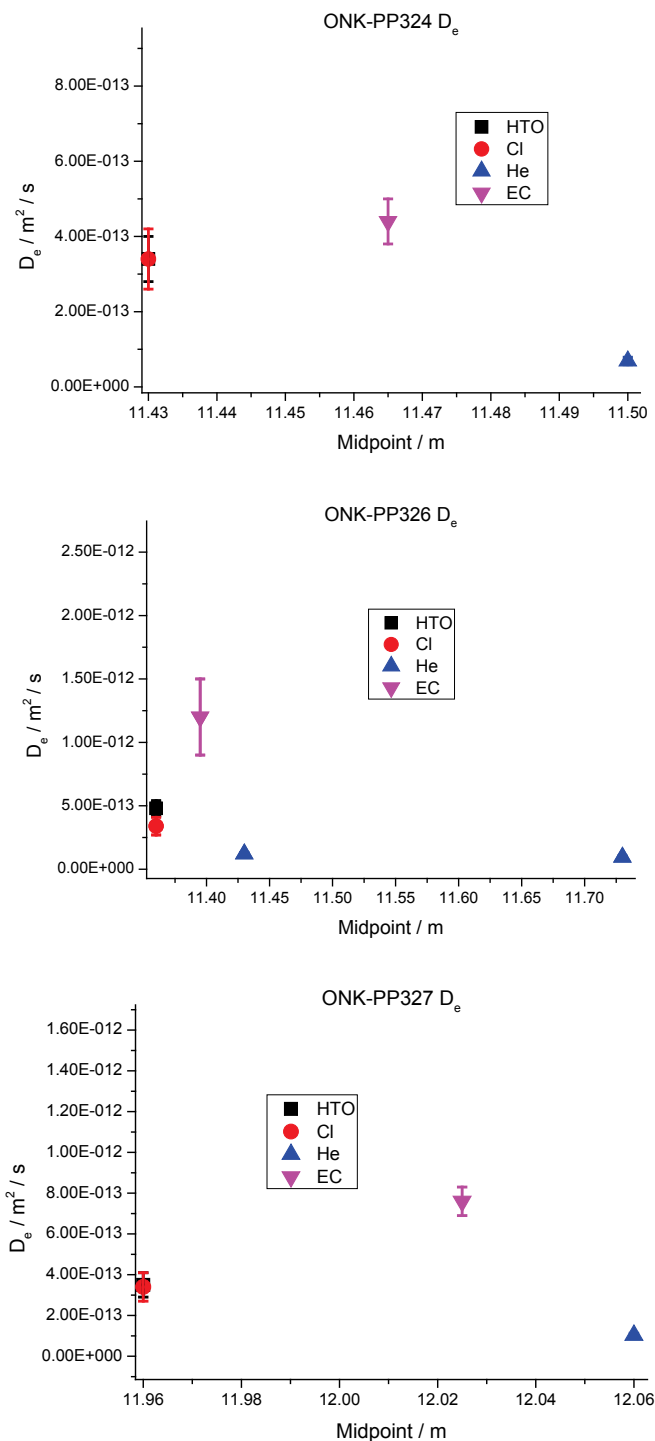
Figure 10. *All diffusivity results for the TDE samples using the water phase (HTO and Cl) and the gas phase (He) through-diffusion experiments, and electrical conductivity measurements (EC).*
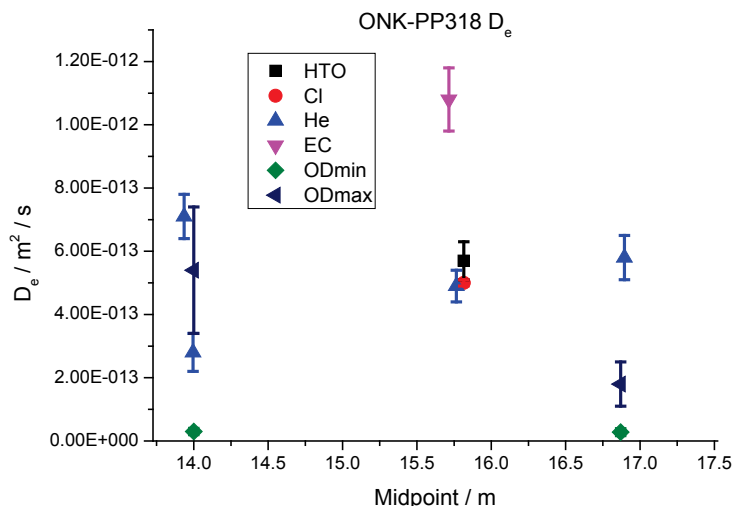
Figure 11. All diffusivity results for the PGR samples using the water phase (HTO and Cl) and the gas phase (He) through-diffusion experiments, electrical conductivity measurements (EC), and out-diffusion experiments (OD).

The PGR samples behaved, as expected, differently than the VGN samples of two previous groups (see Fig.11). No Knudsen diffusion was observed as the gas phase results were in accordance with the water phase results. The effect of anion exclusion was negligible, as the results for Cl and HTO were almost identical. The single electrical conductivity measurement gave an effective diffusion coefficient that was about a factor of two larger than the through-diffusion experiments using HTO as the tracer on a nearby PGR sample. The out-diffusion measurements were in fairly accordance with the other methods. Furthermore, the differences between the minimum and maximum values represent the rock heteroneineity in the grain size scale.

Results for the other samples were somewhere between the other three groups (see Fig. 12). The other samples consisted of VGN with changeable amounts of pegmatitic parts. No Knudsen diffusion was observed but anion exclusion clearly affected the results in those samples which did not contain any pegmatitic parts. The other samples were mixtures of PGR and VGN which could explain the inconsistencies observed in the anion exclusion and Knudsen diffusion behaviour between the sample groups. The electrical conductivity and out-diffusion measurements gave results that were in fair agreement with the other methods one sample.
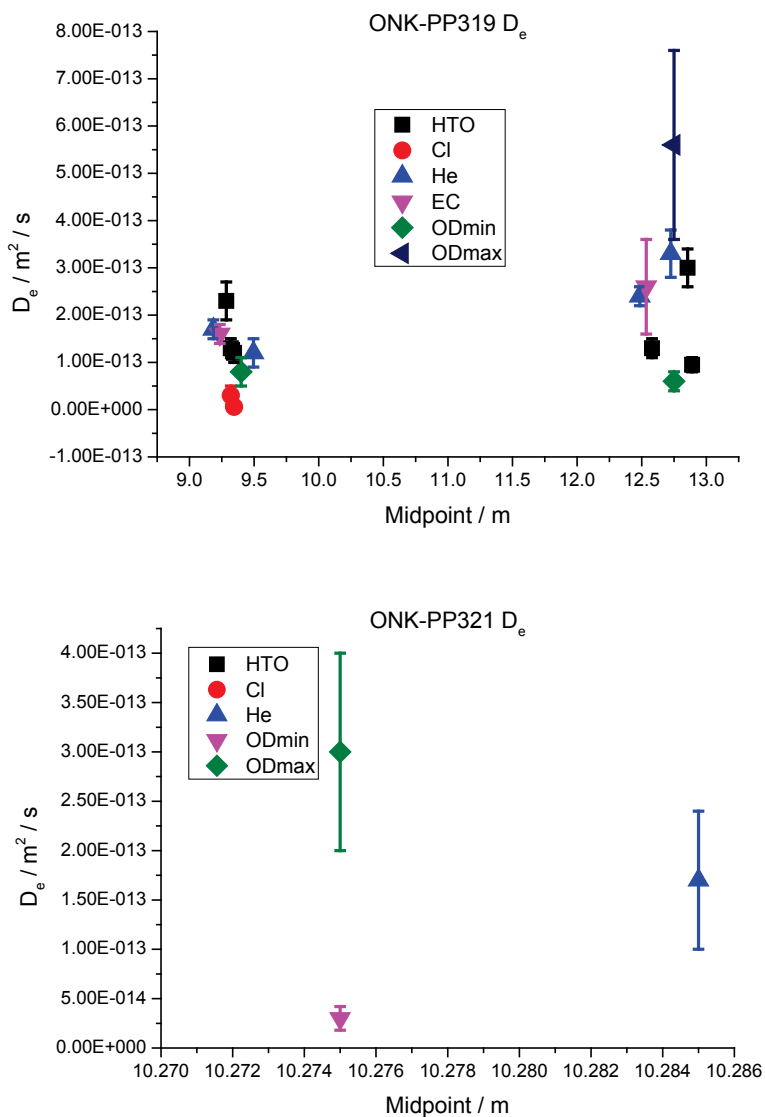
Figure 12. All diffusivity results for the other samples using the water phase (HTO and Cl) and the gas phase (He) through-diffusion experiments, electrical conductivity measurements (EC), and out-diffusion experiments (OD).

4 CONCLUSIONS

Overall, the through-diffusion measurements in the water and gas phases proved to be robust and reliable and provided values that were quite close to each other (see Table 6). The values from the through-diffusion experiments using HTO and ^{36}Cl were found to be in good agreement with previously reported values for VGN and PGR samples from Olkiluoto area (Smellie et al., 2014). The effective diffusivity was smaller for ^{36}Cl than HTO in the VGN samples. The difference cannot be explained only by the difference of diffusion coefficients in free water. A process like anion exclusion must have hindered the diffusion of ^{36}Cl ions. For some VGN samples the diffusivities obtained with the He gas method were smaller than those obtained in the water phase due to Knudsen diffusion. For the PGR samples no significant difference could be observed between different tracers, or between water and gas phase results.

Table 6. *The average effective diffusion coefficients for all samples types with different methods determined as error weighted averages.*

	Method	WPDE samples (VGN)	TDE samples (VGN)	PGR samples	Other samples (VGN)	Smellie et al. (2014)	
						VGN	PGR
$D_e \times 10^{-13}$ m^2/s	HTO	1.7 ± 0.2	3.9 ± 0.4	5.7 ± 0.7	1.3 ± 0.1	1.0 ± 0.4	7.7 ± 2.7
	^{36}Cl	0.05 ± 0.03	3.4 ± 0.5	5.0 ± 1.0	0.07 ± 0.03	0.2 ± 0.2	5.1 ± 2.3
	He-gas	0.51 ± 0.03	1.0 ± 0.1	5.0 ± 0.3	2.0 ± 0.2	-	-
	EC	3.4 ± 1.1	5.9 ± 0.5	11 ± 1	1.6 ± 0.2	-	-
	Out-diff	0.6 ± 0.3	-	2.9 ± 0.5	1.0 ± 0.3	1.3 ± 1.2	3.6 ± 1.3

The out-diffusion measurements also provided results close to those obtained with the through-diffusion measurements. They also provided information that cannot be obtained with the through-diffusion measurements, as the different components of the rock with different transport properties affect different parts of the out-diffusion curve, giving information on transport properties on different lengt scales and grain scale heterogeneities that dominate the out-diffusion curves at different time scales. As the diffusivity obtained from the through-diffusion measurements is a combination of two components, it was to be expected that the lower component was below most values obtained from the through-diffusion measurements and the higher component was above most values obtained from the through-diffusion measurements. The PGR samples had a clear two component behavior, which had already been observed in the gas phase matrix diffusion measurements earlier (e.g. Eichinger et al. 2010). The values given in Table 6 are given according to the dominant components as they are the ones that are likely seen in the through-diffusion measurements in this length scale.

The electrical conductivity measurement gave effective diffusivities that, on average, were a factor of about two larger than the data obtained by the through-diffusion measurements in the water phase, using HTO as the tracer. This is consistent with results from previous comparisons between the methods done on similar rock samples (Ohlsson 2000, Byegård et al. 2008), except for the fact that less anion exclusion was expected in those samples. A correlation between the ionic strength of the electrolyte and the estimated effective diffusion coefficient was expected based on the hypothesis that changing the ionic strength would affect the thickness of the electrical double layer at the mineral surfaces and thus affect the transport of anions in the pore network. The method did not substantiate this hypothesis in a clear manner, but it is questionable if the method is sensitive enough to the impact of anion exclusion to shed light on this matter. The data presenting the total rock conductivities as a function of conductivity of solution were not completely linear as one could expect if the diffusion double layer would not change enough due to differences in the ionic strength of the solution. However, the non-linearity arises from experimental fluctuation and is not in the direction that the electrical measurements could confirm the presence of anion exclusion. The electrical conductivity method seems to be less reliable than the through-diffusion measurements. However, it can offer a rough estimate of the effective diffusion coefficient much faster than the water phase through-diffusion experiments, and the method is relatively easy to implement in situ and thus remains a promising method considering the results obtained here.

REFERENCES

Brace W.F., Orange A.S., 1968. Further Studies of the Effects of Pressure on Electrical Resistivity of Rocks, Journal of geophysical research 73(16), 5407–5420.

Byegård, J., Selnert, E., Tullborg, E.-L., 2008. Bedrock transport properties. Data evaluation and retardation model. Site descriptive modelling, SDM-Site Forsmark. SKB R-08-98, Svensk Kärnbränslehantering AB.

Corey, J. C., Nielsen, D. R., Biggar, J. W., 1963. Miscible Displacement in Saturated and Unsaturated Sandstone. Soil Sci. Soc. Am. J. 27, 258–262.

Eichinger, F.L., Waber, H.N., Smellie, J.A.T., 2006. Characterisation of Matrix Pore Water at the Olkiluoto Investigation Site, Finland. Posiva Working Report 2006-103, Posiva Oy, Eurajoki, Finland.

Eichinger, F., Hämmerli, J., Waber, H.N., Diamond, L.W., and Smellie, J.A.T., 2010. Characterisation of Matrix Pore Water and Fluid Inclusions in Olkiluoto Bedrock from Drilling OL-KR47, Posiva Working Report 2010-58, Posiva Oy, Eurajoki, Finland.

Eichinger, F., Hämmerli, J., Waber, H.N., and Diamond, L.W., 2013. Chemistry and Dissolved Gases of Matrix Pore Water and Fluid Inclusions in Olkiluoto Bedrock From Drillhole ONK-PH9. Posiva Working Report 2011-63, Posiva Oy, Eurajoki, Finland.

Hartikainen, K., Väätäinen, K., Hautojärvi, A., Timonen, J., 1994. Further development and studies of gas methods in matrix diffusion. In: MRS Proceedings 333, 821–826.

Hartikainen, K, Hautojärvi, A., Pietarila, H., Timonen, J., 1995. Diffusion measurements on crystalline rock matrix. In: Murakami, T., Ewing, R. (eds.) MRS Proceedings 353: Scientific Basis for Nuclear Waste Management XVIII, 435–440.

Hartikainen, J., Hartikainen, K., Hautojärvi, A., Kuoppamäki, K., and Timonen, J., 1996. Helium gas methods for rock characteristics and matrix diffusion. Posiva Report 96–22, Posiva Oy, Eurajoki, Finland.

Hartikainen, K., Hartikainen, J., 1998. Posiva's site investigations in Olkiluoto, Kivetty, Romuvaara and Hästholmen by He-gas methods in 1997. Posiva Working Report 98–17e, Posiva Oy, Eurajoki, Finland.

Ikonen, J., Sammaljärvi, J., Siitari-Kauppi, M., Voutilainen, M., Lindberg, A., Kuva, J., Timonen, J., 2015. Investigation of Rock Matrix Retention Properties, Supporting laboratory studies I: Mineralogy, porosity and pore structure, Posiva Working Report 2014-86, Posiva Oy, Eurajoki, Finland.

Johansson, H., Siitari-Kauppi, M., Skålberg, M., Tullborg, E.L., 1998. Diffusion pathways in crystalline rock – examples from äspö-diorite and fine-grained granite. J. Contam. Hydrol. 35, 41–53.

Kaukonen, V., Hakanen, M., Lindberg, A., 1997. Diffusion and sorption of HTO, Np, Na and Cl in rocks and minerals of Kivetty and Olkiluoto, Posiva Working Report 97-07, Posiva Oy, Eurajoki, Finland.

Klinkenberg, L. J., 1941. The permeability of porous media to liquids and gases. Drill. Prod. Pract., 200–236.

Kuva, J., Siitari-Kauppi, M., Lindberg, A., Aaltonen, I., Turpeinen, T., Myllys, M., Timonen, J., 2012. Microstructure, porosity and mineralogy around fractures in Olkiluoto bedrock. Eng. Geol. 139-140, 28–37.

Kuva, J., Voutilainen, M., Kekäläinen, P., Siitari-Kauppi, M., Timonen, J., and Koskinen, L., 2015. Gas phase measurements of porosity, diffusion coefficient, and permeability in tock samples from Olkiluoto bedrock, Finland, Transp. Porous Media 107(1), 187–204.

Kuva, J., Voutilainen, M., Kekäläinen, P., Siitari-Kauppi, M., Sammaljärvi, J., Timonen, J., Koskinen, L., 2016. Gas phase measurements of matrix diffusion in rock samples from Olkiluoto bedrock, Finland. Transp. Porous Media 115(1), 1–20.

Kärki, A., Paulamäki, S., 2006. Petrology of Olkiluoto. Posiva Report 2006-02, Posiva Oy, Eurajoki, Finland.

Löfgren, M., Neretnieks, I., 2006. Through-electromigration: A new method for investigating pore connectivity and obtaining formation factors. J. Contam. Hydrol. 87, 237–252.

Löfgren, M., 2015. Artefacts associated with electrical measurements of the rock matrix formation factor, SKB R-14-20, Svensk Kärnbränslehantering AB, Stockholm, Sweden.

Neretnieks, I., 1980. Diffusion in the rock matrix: an important factor in radionuclide retardation?, J. Geophys. Res. 85(B8), 4379–4397.

Ohlsson, Y., 2000. Studies of ionic diffusion in crystalline rock. Ph.D. thesis. Royal Institute of Technology, Stockholm, Sweden.

Poteri, A., Nilsson, K., Andersson, P., Siitari-Kauppi, M., Helariutta, K., Voutilainen, M., Kekäläinen, P., Ikonen, J., Sammaljärvi, J., Lindberg, A., Byegård, J., Skålberg, M., Kuva, J., Timonen, J., Koskinen, L., 2018. The first matrix diffusion experiment in the water phase of the REPRO project: WPDE1, Posiva Working Report 2017-23, Posiva Oy, Eurajoki, Finland.

Sammaljärvi, J., Ikonen, J., Voutilainen, M., Kekäläinen, P., Lindberg, A., Siitari-Kauppi, M., Pitkänen, P., Koskinen, L., 2016. Chloride diffusion in pore water in Olkiluoto veined gneiss and pegmatitic granite from a structural perspective. MRS advances 61(1), 4047–4052.

Sammaljärvi, J., Ikonen, J., Voutilainen, M., Kekäläinen, P., Lindberg, A., Siitari-Kauppi, M., Pitkänen, P., Koskinen, L., 2017. Multi-scale study of the mineral porosity of veined gneiss and pegmatitic granite from Olkiluoto, Western Finland, Journal of Radioanalytical and Nuclear Chemistry 314, 1557–1575.

Siitari-Kauppi, M., Hellmuth, K.-H., Lindberg, A., Huitti, T., 1994. Diffusion in homogeneous and heterogeneous rock matrices. A comparison of different experimental approaches. Radiochim. Acta 66/67, 409–414.

Smellie, J. (ed), Pitkänen, P., Koskinen, L., Aaltonen, I., Eichinger, F., Waber, N., Sahlstedt, E., Siitari-Kauppi, M., Karhu, J., Löfman, J., Poteri, A., 2014. Evolution of the Olkiluoto Site: Palaeohydrogeochemical Considerations, Posiva Working Report 2014-27, Posiva Oy, Eurajoki, Finland.

Toropainen, V., 2012. Core Drilling of REPRO Drillholes in ONKALO at Olkiluoto 2010-2011, Posiva Working Report 2012-26, Posiva Oy, Eurajoki, Finland.

Valkiainen, M., Aalto, H., Lindberg, A., Olin, M., Siitari-Kauppi, M., 1995. Diffusion in the matrix of rocks from Olkiluoto: The effect of anion exclusion, YJT-95-20, Imatran Voima Oy, Vantaa, Finland.

Voutilainen, M., Poteri, A., Helariutta, K., Siitari-Kauppi, M., Nilsson, K., Andersson, P., Byegård, J., Skålberg, M., Kekäläinen, P., Timonen, J., Lindberg, J., Pitkänen, P., Kemppainen, K., Liimatainen, J., Hautojärvi, A., Koskinen, L., 2014. In-situ experiments for investigating the retention properties of rock matrix in ONKALO, Olkiluoto, Finland, Proceedings of the Waste Management 2014 Conference (14258), March 2–6, 2014, Phoenix, Arizona, USA.

Voutilainen, M., Ikonen, J., Sammaljärvi, J., Kuva, J., Lindberg, A., Siitari-Kauppi, M., Koskinen, L., 2016. Through diffusion study on Olkiluoto veined gneiss and pegmatitic granite from a structural perspective. MRS advances 1(61), 4041–4046.

Voutilainen, M., Ikonen, J., Kekäläinen, P., Sammaljärvi, J., Siitari-Kauppi, M., Lindberg, A., Kuva, J., Timonen, J., 2017. Matrix Pore Water study on REPRO samples, Posiva Working Report 2017-22, Posiva Oy, Eurajoki, Finland.

Waxman, M. H., Smits, L. J. M., 1968. Electrical conductivities in oil-bearing shaly sands, Society of Petroleum Engineering Journal 8 (2), 107–122.

Väätäinen, K., Timonen, J., Hautojärvi, A., 1993. Development of a gas method for migration studies in fractured and porous media. In: MRS Proceedings 294, 851–856.